

FLEXIBLE PLATE SUPERSONIC WIND TUNNEL FLOW CORRECTION
TO ACCOUNT FOR PLATE ELASTIC PROPERTIES

Thesis by
Patrick S. Chase

In Partial Fulfillment of the Requirements
For the Degree of
Aeronautical Engineer

California Institute of Technology
Pasadena, California

1950

ACKNOWLEDGMENTS

The writer is indebted to Drs. A. E. Puckett and H. T. Nagamatsu for their guidance during this investigation. Valuable assistance was also rendered by Mrs. P. S. Chase and Mrs. Melba Nead in computing and by Miss Shirley Woodbury in typing and assembling the final manuscript.

ABSTRACT

A method of correcting the static pressure distribution in the working section of a supersonic wind tunnel with flexible nozzle walls is investigated, in order to account for the discrepancy between the theoretical nozzle wall shape and the actual wall shape due to its elastic properties.

The method of correction is described and an example for an existing wind tunnel is carried out. It is shown that the method of correction is not successful due to the inadequate accuracy of the data from physical measurements and due to the nature of the equations which must be solved. While the former difficulty could possibly be avoided, the latter is considered to be inherent in the method.

Suggestions and criticisms are offered and some results of the investigation regarding correction of the actual wind tunnel static pressure distributions are mentioned.

TABLE OF CONTENTS

<u>Part</u>	<u>Title</u>	<u>Page</u>
I.	Introduction	1
II.	Theory of Nozzle Shape Correction	5
III.	Computational Procedure	11
IV.	Comparison With a Second Correction Technique	14
V.	Discussion of Results	17
	A. General	17
	B. As Applied to the Jet Propulsion	
	Laboratory 12" Supersonic Wind Tunnel	19
	Appendix	22
	References	28
	Tables	29
	Figures	32

LIST OF FIGURES

<u>Figure No.</u>		<u>Page</u>
1.	J.P.L. 12" Supersonic Wind Tunnel Configuration	32
2.	Comparison of Theoretical Design Wall Slope and Actual Wall Slope	33
3.	Influence Region and Mach Waves	34
4.	Wall Slope Influence Curves for Unit Deflection of the Adjustment Points	35
5.	Desired Slope Correction	36
6.	Mach Wave Reflection Curves	37
7.	Graphical Integration $\int_0^{18} \lambda'_0 \lambda'_0 dx$	38
8.	Graphical Integration $\int_0^{18} \lambda'_1 \lambda'_5 dx$	39
9.	Graphical Integration $\int_0^{18} \lambda'_2 \lambda'_4 dx$	40
10.	Comparison Desired Slope Correction and that Actually Obtained	41
11.	Comparison of Two Methods of Flow Distribution Correction	42

LIST OF TABLES

<u>Table No.</u>		<u>Page</u>
I.	Nozzle Coordinates	29
II.	Simultaneous Equations Governing the Motion of Six Adjustment Points	30
III.	Numerical Simultaneous Equations for $M = 2.537$ Nozzle, J.P.L. 12" Supersonic Wind Tunnel	31

LIST OF SYMBOLS

a_i	Displacement of the i^{th} adjustment point
E	Modulus of elasticity of flexible plate
I	Moment of inertia of flexible plate cross-section about its neutral axis
l	Chord length between two adjacent adjustment points
M	Mach number
p	Free stream static pressure
p_o	Free stream total pressure
T	Bending moment
x	Nozzle longitudinal coordinate
x_o	Nozzle longitudinal coordinate at upstream end of first influence region, Figure 3
y	Nozzle transverse (vertical) coordinate
$\Delta\alpha_n$	Angle at n^{th} adjustment point between chord lines from the $(n - 1)$ and $(n + 1)$ adjustment points
$\theta_{n, n+1}$	Slope of chord between n^{th} and $(n + 1)^{\text{th}}$ adjustment points
γ	Ratio of specific heats = 1.4
λ	Nozzle wall slope (radians)
λ_c	Desired nozzle wall slope correction
$\lambda_i(x)$	Slope change at point x due to displacement of the i^{th} jack
$\lambda'_i(x_w)$	Effective slope influence curve at x_w for unit displacement of i^{th} jack

LIST OF SYMBOLS (continued)

- ()_w Refers to first upstream intersection with nozzle wall of a Mach wave from a point on the tunnel axis in the working section, Figure 3
- ()_{1w} Refers to second upstream intersection with nozzle wall of a Mach wave from a point on the tunnel axis in the working section, Figure 3
- ()_{2w} Refers to third upstream intersection with nozzle wall of a Mach wave from a point on the tunnel axis in the working section, Figure 3

I. INTRODUCTION

The problem of obtaining a uniform flow distribution in the working section of a wind tunnel, whether subsonic or supersonic, is always a primary design consideration.

The innovation of supersonic wind tunnels with flexible nozzle walls to allow variation of flow Mach number at the working section has presented an additional hindrance in obtaining satisfactory flow distribution. The difficulty arises from the elastic properties of the plates which form the flexible walls of the nozzle.

In general, to obtain the desired uniformity of flow in a supersonic tunnel, the nozzle shape can be determined by any one of several accepted methods, (Ref. 1) based on perfect fluid theory. Then a boundary layer correction is applied in order to account for the real fluid effects. The flexible walls of the nozzle are then adjusted by means of their supports to correspond to the desired shape. If irregularities in the experimentally measured flow distribution are found, there are two possible sources of error. Variations may be due to errors in the aerodynamic assumptions involved in the shape computation or due to the fact that the flexible plate does not assume the desired contour although it is supported at a finite number of points exactly on the contour. Since much study has already been applied to the aerodynamic problems involved, the purpose of this paper will be to investigate the

wall elastic problem.

The flexible plate will exactly assume the desired aerodynamic shape only if, (1) the aerodynamic shape is such that its curvature is identical to that which the plate will assume due to its elastic properties or (2) if there are an infinite number of adjustable supports. Condition (2) is obviously impossible and with the present methods of design, condition (1) is not fulfilled.

In addition, the discrepancies between desired shape and actual elastic shape are accentuated by the fact that the nozzle is often too short to allow a continuous curvature distribution along the plate in the initial design. Some of the reasons for short nozzles are:

1. To prevent excessive boundary layer growth
2. Space requirements
3. Structural requirements on the tunnel frame
4. Economics

For these reasons it would appear that a method of minimizing the errors due to plate elastic properties would be useful. The problem is then to determine the best settings for the plate supports in order that the variation of desired from actual plate shape will be a minimum over the critical portion of the nozzle.

To demonstrate the correction method described in Section II, the 12" Supersonic Wind Tunnel of the Jet Propulsion Laboratory, California Institute of Technology, was used as a model. As a matter of fact, it

was in an effort to optimize the experimentally measured static pressure distributions of this facility, and those of a future more elaborate installation, that the present investigation was undertaken.

The 12" tunnel is capable of continuous operation for Mach numbers in the range of 1.2 to 3.0. Above a Mach number of 2.2, the working section dimensions are 9" x 12" because of the limits imposed by the present compressor plant. Since static pressure distributions at the higher Mach numbers were found to be less regular than those at lower Mach numbers, the nozzle contour for Mach number 2.537 was chosen for the investigation. The coordinates for this nozzle are presented in Table I.

The nozzle sidewalls are 12" apart, flat and parallel, with the top and bottom wall contours formed from flexible steel plates. The pertinent features of the flexible nozzle plates are shown in Figure 1. Each plate is 12" wide and 1/4" thick with twelve jack connections available for positioning it. In addition, the plate ordinate and slope at station $x = 0$ are adjustable. Due to the limitations imposed by the plate strength, aerodynamic considerations, and the tunnel frame dimensions, the basic nozzle shape was composed of a circular arc segment through the throat to the maximum expansion angle, a straight line segment, and the remainder of the curve to the working section was an analytic shape designed to convert a supersonic source flow into a uniform parallel flow. To this basic shape, a non-analytic boundary layer correction was added between the throat and the working section, (Ref. 2); thus, removing the possibility of expressing

this portion of the nozzle with simple mathematical expressions. It is obvious that this shape has sharp discontinuities of curvature in the vicinity of the inflection point which cannot be reproduced by the flexible plate with its continuous moment distribution.

II. THEORY OF NOZZLE SHAPE CORRECTIONS

If a uniform elastic plate is supported at a finite number of points situated on a given contour, the elastic shape which the plate will assume can be computed by a relaxation method; in this case the Hardy-Cross method. The slope distribution is of principle interest because flow disturbances originate essentially from changes in the wall slope.

Due to the fact that local static pressure disturbances are directly proportional to local wall slope, the comparison of theoretical design wall slope and actual elastic wall slope, (cf. Figure 2) gives a measure of the pressure disturbances which can arise due to elastic effects. Although the difference for the J.P.L. 12" Supersonic Wind Tunnel appears very small in Figure 2, the constant of proportionality is such that errors in the static pressure distribution in the working section of several percent are caused. This is a large amount when it is considered that variations from the mean pressure level of $\pm 0.25\%$ or less were desired for this precision tunnel.

Assuming a two-dimensional flow, conditions at each point on the test section axis are influenced by the nozzle wall slope at points lying on the upstream extension of the Mach wave, from the original point, and its reflections extended back to the nozzle throat as shown in Figure 3. Since each point on the test section axis is influenced directly by a

point in the "first influence region", Figure 3, it is reasonable to attempt correction of the static pressure distribution by changes in this region. The displacement of any jack in this region (or any other) will cause deflections to occur all along the length of the plate. This slope-change pattern can be computed for each jack by elastic theory procedure and will be referred to as the slope-influence curve. Such curves for the support points of interest in the J.P.L. 12" Supersonic Wind Tunnel are shown in Figure 4. Any corrections to the slope, which are desired to alter the static pressure distribution on the working section axis, must be obtained from linear combinations of these influence curves. The problem becomes that of determining the slope correction in the first influence region which will arise due to the plate elasticity, and then to determine the best combination of influence curves to obtain this correction, (cf. Ref. 3).

A symmetric slope change of $+\lambda$ on the top and bottom walls (i.e. both moved out) will result in a static pressure change of

$$\frac{\Delta p}{p} = - \frac{2 \gamma M^2}{\sqrt{M^2 - 1}} \lambda$$

without changing the flow inclination on the tunnel axis. Therefore, for a pressure error $\Delta p(x)$ on the axis, the slope correction on the wall at x_w becomes

$$\lambda(x_w) = \frac{\sqrt{M^2-1}}{2 \gamma M^2} \frac{\Delta p(x)}{\rho} \quad (1)$$

This relation will be useful in later comparisons. However, in the present case the slope correction is not based on observed pressure irregularities but on the desired slope correction λ_c determined from Figure 2 and plotted in Figure 5. It must be remembered that the pressure change through a Mach wave retains the same sign upon reflection from a wall. Therefore, the slope change at the second influence point x_{1w} is equivalent to a slope change of the same sign and magnitude at x_w in its effect on the pressure distribution on the working section axis.

Therefore, the actual wall slope corrections which can be obtained within the first influence region are

$$\lambda(x_w) = \sum_i a_i \lambda'_i(x_w)$$

where $\lambda'_i(x_w)$ is the effective influence curve at x_w for unit displacement of i^{th} adjustment point or jack and a_i is the actual displacement of that point. Therefore,

$$\lambda'_i(x_w) = \lambda_i(x_w) + \lambda_i(x_{1w}) + \lambda_i(x_{2w}) + \dots \quad (2)$$

and $x_w, x_{1w}, x_{2w},$ etc., denote the location of upstream intersections of the Mach wave from the point x on the working section axis with the nozzle walls on the first, second, etc., reflections. $\lambda_i(x)$ is the geometrical slope change at x due to displacement of the i^{th} jack.

Suppose $\lambda_c(x_w)$, the desired slope correction, has been determined as in Figure 5 from the plate elastic properties. Let $f(x)$ be the difference between $\lambda_c(x_w)$ and $\lambda(x_w)$, the actual obtainable correction,

$$f(x) = \lambda_c(x_w) - \lambda(x_w)$$

The best correction will be obtained if the average of $f(x)^2$ over the first influence region is a minimum. It is possible to solve for the influence coefficients a_i by minimizing the function R , where

$$R = \int_0^{x_0} [\lambda_c(x_w) - \sum_i a_i \lambda'_i(x_w)]^2 dx$$

To obtain the optimum influence coefficients a_i , set the derivative of R with respect to a_k (the motion of the k^{th} adjustment point) equal to zero and solve for a_k as follows; differentiating R with respect to a_k ,

$$\frac{\partial R}{\partial a_k} = \frac{\partial}{\partial a_k} \int_0^{x_0} [\lambda_c(x) - \sum_i a_i \lambda'_i(x_w)]^2 dx$$

or

$$\frac{\partial R}{\partial a_k} = \frac{\partial}{\partial a_k} \int_0^{x_0} \left[\lambda_c(x_w)^2 - 2\lambda_c(x_w) \sum_i a_i \lambda'_i(x_w) + \left\{ \sum_i a_i \lambda'_i(x_w) \right\}^2 \right] dx$$

However, the only terms which contribute are

$$\frac{\partial R}{\partial a_k} = \left\{ -2\lambda_c(x_w) \lambda'_k(x_w) + 2\lambda'_k(x_w) \sum_i a_i \lambda'_i(x_w) \right\}$$

To prove that this quantity furnishes a minimum when equated to zero, take the second derivative of R with respect to a_k and show that it is positive. Therefore,

$$\begin{aligned} \frac{\partial^2 R}{\partial a_k^2} &= 2 \lambda'_k(x_w) \lambda'_k(x_w) \\ &= 2 \left[\lambda'_k(x_w) \right]^2 \end{aligned}$$

Obviously $\frac{\partial^2 R}{\partial a_k^2}$ is always positive regardless of the sign of $\lambda'_k(x_w)$, so the condition, $\frac{\partial R}{\partial a_k} = 0$, furnishes a minimum and

$$\lambda_c(x_w) \lambda'_k(x_w) = \lambda'_k(x_w) \sum_i a_i \lambda'_i(x_w)$$

Integrate from $x = 0$ to $x = x_0$ and the condition for a_k becomes

$$\int_0^{x_0} \lambda_c(x_w) \lambda'_k(x_w) dx = \int_0^{x_0} \lambda'_k(x_w) \sum_i a_i \lambda'_i(x_w) dx \quad (3)$$

The summation is extended over the number, n , of adjustment points used in the correction. There will be n simultaneous equations for n different values of k . These n simultaneous equations may then be solved for the n values of a_i necessary for the optimum adjustment.

This method is straight forward but involves a great deal of labor in computation if more than a few adjustment points are considered.

III. COMPUTATIONAL PROCEDURE

Although the correction method described in Section II is simple in theory, it involves a rather intricate computational procedure. This procedure will be described in some detail here for the special case of the Mach number 2.537 nozzle contour of the 12" Supersonic Wind Tunnel at the Jet Propulsion Laboratory, California Institute of Technology. Six adjustments will be considered; five involve plate ordinate adjustments and one involves changing the wall slope at Station 0, Figure 1. It was felt that these six adjustments would be sufficient in view of the amount of computational labor involved.

The correction will be discussed in a step-wise fashion with representative tables and curves included. The procedure is as follows:

1. Compute actual moment distribution in the flexible plate by the relaxation method described in the Appendix.
2. Integrate the function $\frac{I}{EI}$ graphically or numerically to obtain a curve of the actual elastic plate slope, Figure 2.
3. Measure graphically on a very large scale curve the slopes of the theoretical design contour and plot as in Figure 2. In this step a scale of 10 cm. on the graph to 1 inch on the actual nozzle is recommended.
4. Take difference between theoretical and actual slope curves to obtain $\lambda_c(x_w)$, the desired correction, Figure 5.

5. Compute influence curves for unit displacement of the adjustment points. (These have been previously computed for the two J.P.L. supersonic tunnels and the method will not be discussed here since it is in accord with normal elastic theory). These curves are plotted on Figure 4.
6. Compute curves of Mach wave upstream wall intersection and reflection points by the method of characteristics for the theoretical nozzle contour with boundary layer correction. Data from the characteristics plot are shown in a more readily useable form in Figure 6.
7. Write equation (3) out in detail for easy visualization of the computational steps involved. Table II presents the six expanded equations which will be used to solve for the optimum displacements of the adjustment points.
8. Compute necessary quantities $\lambda'_i(x_w)$ to place in the equations of Table II from equation (2) and the curves of Figures 4 and 6.
9. Perform multiplications indicated by the equations, Table II.
10. Perform the integrations indicated by Table II, either graphically or by Simpson's rule. A comparison of the two methods, as shown by Figures 7 through 9, proves

either to be of satisfactory accuracy for the representative cases chosen.

11. Set-up the six linear simultaneous equations, Table II, with numerical values. Numerical examples are shown in Table III.
12. Solve these equations for the a_i 's. This is very tedious in the case of six simultaneous equations and solution by automatic computing machines such as International Business Machines or the Consolidated Engineering Company's linear simultaneous equation computer is recommended. In the present case IBM equipment was used.
13. Compute the slope correction curves which can actually be obtained and compare with the desired slope correction λ_c . The comparison obtained in the present example is shown in Figure 10 for two independent computations by the method described.

IV. COMPARISON WITH A SECOND CORRECTION TECHNIQUE

The results of Section III have shown that the method of correction which has been described is unsuccessful due to excessive scatter in the correction data obtained. The probable reasons for this condition are discussed in Section V and are found to be arithmetic. However, it is of value to consider the results that this method of correction would have produced if successful and to compare them with the results produced by another correction method.

This second method is one which has actually been used on the J.P.L. 12" Supersonic Wind Tunnel with some success. Briefly it consists of a short cut method by which the amount of labor involved in the method previously described, and hereafter referred to as Method 1, is reduced. In addition, Method 2 undertakes the correction of flow deviations due to effects other than elastic. By Method 2 no attempt is made to obtain the best average correction but instead an attempt is made to correct the experimentally measured pressure distribution at a finite number of points. By using n adjustment points, the value of static pressure at $n + 1$ points can be brought into agreement at an undetermined level. The absolute value of this level is unimportant since if the pressure distribution can be made to be satisfactory, the flow Mach number can easily be determined. Then by interpolating between adjustment point settings for various successfully corrected pressure distributions, any

desired flow Mach number can be obtained with reasonable assurance that the accompanying pressure distribution will be satisfactory.

The result of applying Method 2, using four adjustment points, is shown on Figure 11 as compared to the original experimentally measured static pressure distribution and the results of correction by Method 1 if it had been successful. It may be seen that in the region between $x = 0$ and $x = -13$, the first experimentally measured curve has been brought into good agreement at an average level of Mach 2.576 by correction Method 2. However, the region between $x = 0$ and $x = +9$ has not been improved appreciably. It can be shown from the curves of Mach wave reflection points, Figure 6, that this region corresponds closely to the region of inflection of the nozzle wall.

It is also evident that the correction of plate elastic properties by Method 1, if successful, improves the region from $x = -2$ to $x = +9$ to an almost constant value although no improvement is shown in the region $x = -2$ to $x = -13$.

These comparisons show that the plate elastic properties are responsible for the irregularities in pressure distribution produced in the neighborhood of the inflection point (i.e. $x = 0$ to $x = +9$). Irregularities downstream of $x = 0$ are apparently due to the aerodynamic design and are most likely involved in the boundary layer correction which was arbitrarily chosen with the exception of two computed points, one at the nozzle throat and the other at the nozzle exit. The boundary layer

correction was applied in this fashion because insufficient theory and experimental data existed to warrant a more exact computation.

The correction of Method 2 is useful because it attempts correction of all sources of flow irregularities and embodies a minimum of computational effort. It must be applied however after experimental data have been obtained and is not suitable for the correction of the irregularities of flow due to wall elastic properties. Method 1 is desirable (if it could be made practical) because it allows correction for the plate elastic properties before test data is available. It could also be utilized in the fashion of Method 2 to make a correction to experimentally measured data so that all sources of pressure irregularity could be improved. Method 1 is undesirable because the amount of labor involved in computation is appreciable if a large number of adjustment points is considered. For instance, if the number of adjustment points is increased from six to eight the amount of work involved in obtaining a solution is approximately doubled.

V. DISCUSSION OF RESULTS

A. General

A method for the correction of flow irregularities due to the elastic properties of flexible nozzle walls has been presented. It has been shown that the method is unsuccessful when applied in the specific case of the Jet Propulsion Laboratory 12" Supersonic Wind Tunnel. In view of the scatter on both sides of the desired result, Figure 10, there are two possible reasons that the method fails;

1. The data from physical measurements such as the graphical (or approximate) integration of the integrals, Table II, are not sufficiently accurate.
2. The solution of these linear simultaneous equations, Table II, is not possible with sufficient accuracy because multiples and differences of large numbers are involved.

The difficulty described in (1) above could be circumvented if the boundary layer correction applied to the nozzle was made an analytic function. Even though the validity of the boundary layer correction would not be improved, it would allow the entire computational procedure to be approached on an analytic basis with a consequent increase in accuracy of computation. The difficulty mentioned in (2) presents a more imposing problem since in the present case IBM computation to 10

significant figures was used in an attempt to secure sufficient accuracy in this portion of the solution. However, multiplication of the original matrix by the inverse matrix of the solution showed appreciable errors to be present in the IBM computation. An encouraging note is seen in Figure 10 where the data from the second set of computations are obviously much better than those of the first independent computation. This fact might indicate that the difficulty (1) is predominant and that the difficulty (2) may not be too serious. Difficulty (2) could be checked by having independent computations of the same matrix, Table III, carried out by IBM in order to compare the difference in slope correction, λ_c , which is obtained. If the IBM computing error was proven to cause a substantial portion of the discrepancy, there still remains the possibility that an average of many IBM computations would give useable results since the IBM errors are non-systematic.

In view of the results discussed in Section V and shown in Figure 11, it appears that this method of correction would be a useful tool in flexible nozzle design if it were perfected. Whether or not the labor involved in the computation is warranted by the results which are theoretically obtainable is a question which must be weighed for the case at hand. It is believed, however, that further investigation into the possibility of perfecting the method is desirable.

An important result of the investigation is that care should be taken to design flexible nozzles to have as nearly continuous curvature (or

moment distribution) as possible. The deviation from desired nozzle wall shape and actual wall shape due to the flexible plate elastic properties can easily be excessive. The continuous curvature criterion was previously recognized as important from an aerodynamic standpoint and becomes increasingly important in the light of the present study.

It is suggested that a fruitful field for further research would be the aerodynamic design of flexible wall nozzles having a continuous curvature compatible with that required by the flexible plate, i.e., aerodynamic design to suit the required elastic conditions. It is possible that some parameters such as the nozzle length to working section height ratio, the nozzle throat location or the plate characteristics will control the selection of a compatible design compromise.

B. As Applied to the Jet Propulsion Laboratory 12" Supersonic Wind Tunnel.

Several specific conclusions were arrived at concerning the J.P.L. 12" Supersonic Wind Tunnel, although they were supplemental to the purpose of the investigation. Since the work was initiated primarily for the benefit of the J.P.L. facilities, it is appropriate to include these results here.

1. In the $M = 2.537$ nozzle shape which was considered, the boundary layer correction which was incorporated was probably responsible for the hump in the original pressure distribution curves between $x = -2$ and $x = -13$. The valley from $x = -2$ to $x = +9$ was probably due to the plate elastic properties and is not easily corrected by Method 2 which has been

used thus far in the correction of nozzle shapes for this facility.

2. A revised boundary layer correction might be estimated from the fact that the theoretical correction which could be chargeable to the plate elastic properties does not change the shape of the pressure distribution curve appreciably between $x = -2$ and $x = -10$. Therefore, this irregularity lies in the aerodynamic design and most probably is due to the boundary layer assumptions (since this subject is least understood in supersonic flow). This revised boundary layer correction would be useful in the design of the J.P.L. 20" Supersonic Wind Tunnel which is being constructed. It should allow a better pressure distribution to be obtained initially and thus improve the convergence of the flow correction procedure.

3. The correction produced by Method 2 should be satisfactory at $M = 2.537$ in the region which a model normally occupies (i.e., $x = -2$ to $x = -14$) but may be less effective when the Mach number is such that the inflection point of the flexible plates influences this region.

4. A possible means of avoiding the entire difficulty due to the elastic effects of the plate would be to arrange the upstream hinge points of the flexible plates so that they are closer to the tunnel axis. This would allow redesign of the nozzle shapes to avoid discontinuous curvatures and would decrease the discrepancies due to elastic effects. It is believed that this procedure might be physically possible without great expense, although considerable time and labor would be required to

redesign the nozzle shapes and to recalibrate the tunnel.

APPENDIX

The exact shape which the flexible plate will assume is statically indeterminate and must be computed by a relaxation method, essentially the Hardy-Cross method, (cf. Ref. 4 and 5). Puckett has demonstrated the application of this method to the problem at hand in Ref. 6.

The flexible plate can be forced into an arbitrary initial shape which is known by the application of a given moment at each of the joints. If the initially chosen shape is reasonably close to the final true shape, a series of adjustments of the assumed moment distribution will eliminate the external moments and result in the correct free shape.

In order to start with a reasonable initial moment distribution, the plate is assumed broken at every joint in such a way that the slope is continuous at the joint. Let the angle between the chords of two adjacent segments at joint n be $\Delta\alpha_n$ as in Figure a.

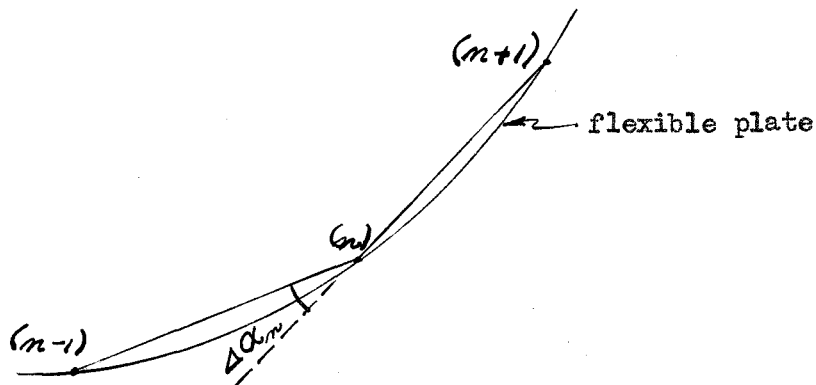


Figure a

A reasonable initial shape will be produced if each segment is bent so that it makes an angle $\frac{\Delta\alpha_n}{2}$ with its own chord at the n^{th} joint. This shape can be attained by applying a moment T_n' at the left end of segment $(n, n+1)$ and a moment T_{n+1} at the right end of segment $(n, n+1)$. From the simple elastic beam theory for a simply supported beam with loads as shown in Figure b,

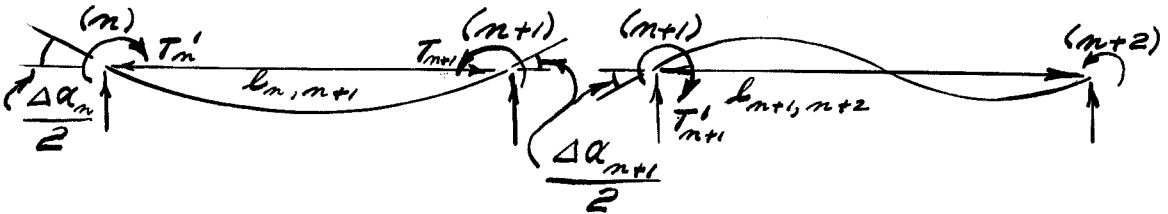


Figure b

the angle $\frac{\Delta\alpha_n}{2}$ is produced by T_n' and T_{n+1} as follows

$$\frac{\Delta\alpha_n}{2} = \frac{T_n' l_{n,n+1}}{3EI} + \frac{T_{n+1} l_{n,n+1}}{6EI}$$

and angle $\frac{\Delta\alpha_{n+1}}{2}$ is

$$\frac{\Delta\alpha_{n+1}}{2} = \frac{T_{n+1} l_{n,n+1}}{3EI} + \frac{T_n' l_{n,n+1}}{6EI}$$

Solving for T_n' and T_{n+1} gives

$$\frac{T_n'}{EI} = \frac{2\Delta\alpha_n - \Delta\alpha_{n+1}}{l_{n, n+1}} \quad (1)$$

$$\frac{T_{n+1}}{EI} = \frac{2\Delta\alpha_{n+1} - \Delta\alpha_n}{l_{n, n+1}} \quad (2)$$

If the ordinates of the joints are given as shown in Figure c and if the slope of a chord $(n, n+1)$ is $\theta_{n, n+1}$,

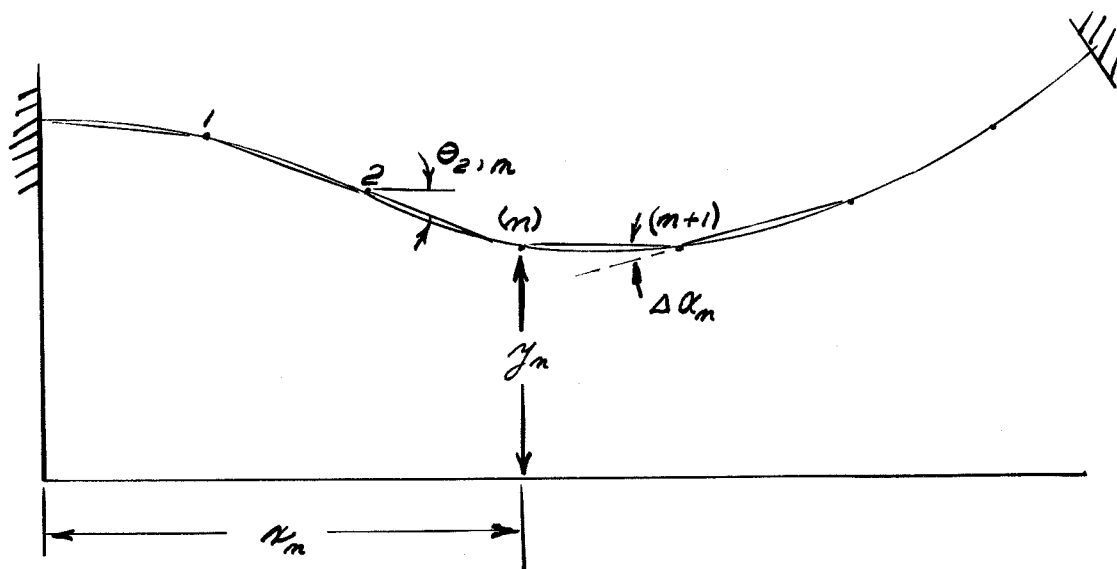


Figure c

the angles between the chords are obtained from

$$\Delta \alpha_m = \theta_{m-1, m} + \theta_{m, m+1}$$

and

$$\tan \Delta \alpha_m = \frac{\tan \theta_{m, m+1} - \tan \theta_{m-1, m}}{1 + \tan \theta_{m, m+1} \tan \theta_{m-1, m}} \quad (3)$$

and therefore,

$$\tan \theta_{m, m+1} = \frac{y_{m+1} - y_m}{h_{m+1} - h_m}$$

$$\tan \theta_{m-1, m} = \frac{y_m - y_{m-1}}{h_m - h_{m-1}}$$

Equations (1), (2), and (3) are sufficient to deform all the segments into the desired initial shape which is taken to be the computed aerodynamic shape for the nozzle. However, the joints at either end of the plate are slightly different since they are effectively cantilevered. By the same procedure as previously used the moments T_0' and T_1 become

$$\frac{T_0'}{EI} = \frac{4\Delta \alpha_0 - \alpha_1}{l_{01}}$$

$$\frac{T_n}{EI} = \frac{2\Delta\alpha_1 - 2\Delta\alpha_0}{l_{01}}$$

We now have the moment distribution necessary to force the plate into the computed aerodynamic shape at the jack points.

These moments are in general not equal on either side of a joint, i.e., $T_n \neq T_n'$. Therefore a redistribution or relaxing of these moments must be made in order to attain the final free elastic shape. Consider all joints fixed except n . At this point $T_n \neq T_n'$ so an external moment $T_n' - T_n$ must be applied to counteract the inequality. If an external moment $\Delta T \neq T_n' - T_n$ is applied, a certain fraction F will act on segment $(n-1, n)$ and the remainder upon segment $(n, n+1)$. The moment T_n is now replaced by $T_n + F\Delta T$ and the moment T_n' by $T_n' - (1-F)\Delta T$. The fraction F can be shown to be

$$F = \frac{\frac{I_{n-1,n}}{l_{n-1,n}}}{\frac{I_{n-1,n}}{l_{n-1,n}} + \frac{I_{n,n+1}}{l_{n,n+1}}}$$

Since the joints $(n-1)$ and $(n+1)$ remained fixed during this procedure of applying ΔT to joint n , additional moments are carried over to points $(n-1)$ and $(n+1)$. It can be shown that the application

of $+ FAT$ to the right end of segment $(n - 1, n)$ induces a moment $- F\frac{\Delta T}{2}$ at the left end of the segment and similarly a moment $+ (1 - F)\frac{\Delta T}{2}$ is induced at the right end of segment $(n, n + 1)$.

This process of releasing a joint and eliminating its unbalance can now be applied to all joints in turn. When the process is complete, a new moment distribution prevails which has smaller differences at the joints than the previous set. These smaller unbalanced moments are then redistributed in the same way and the process is continued until all significant moment difference at the joints disappears. The moment distribution then corresponds to that actually realized in the elastic plate with no external moments applied.

The moment distribution (i.e., curvature) has been computed and by integration the actual true slopes of the elastic plate may be obtained.

REFERENCES

1. Crown, J. C., "Supersonic Nozzle Design", N.A.C.A. Technical Note 1651, June, 1948.
2. Puckett, A. E., "Supersonic Nozzle Design", Journal of Applied Mechanics, Vol. 13, No. 4, 1946.
3. Puckett, A. E., "Design and Operation of a 12" Supersonic Wind Tunnel", Preprint, Institute of Aeronautical Sciences, Summer, 1948.
4. Niles, A. S. and Newell, J. S., "Airplane Structures", Vol. II, Wiley and Son, 1938.
5. Timoshenko, S., "Theory of Elasticity", McGraw Hill, 1934.
6. Puckett, A. E., "Stress and Deflection Analysis of Flexible Nozzle Plate", 1947 (unpublished).
7. Liepmann, H. W. and Puckett, A. E., "Aerodynamics of a Compressible Fluid", Wiley and Son, 1947.

TABLE I

Nozzle Coordinates $M = 2.537$, J.P.L. 12" Supersonic Wind Tunnel

x	y
0	4.5000
1.510	4.4809
2.942	4.4461
4.312	4.4026
5.614	4.3483
6.868	4.2842
8.084	4.2113
9.258	4.1292
10.362	4.0414
11.409	3.9505
12.404	3.8558
13.360	3.7564
14.294	3.6489
15.172	3.5416
16.012	3.4300
16.813	3.3187
17.578	3.2044
23.484	2.2990
25.000	2.0863
27.500	1.8090
30.000	1.6236
32.500	1.5314
33.727	1.5201 (throat)

TABLE II

SIMULTANEOUS EQUATIONS GOVERNING THE MOTION OF

SIX ADJUSTMENT POINTS, a_0 THRU a_5

$$a_0 \int_0^{x_0} \lambda'_0(x) \lambda'_0(x) dx + a_2 \int_0^{x_0} \lambda'_1(x) \lambda'_0(x) dx + a_3 \int_0^{x_0} \lambda'_3(x) \lambda'_0(x) dx + a_4 \int_0^{x_0} \lambda'_4(x) \lambda'_0(x) dx + a_5 \int_0^{x_0} \lambda'_5(x) \lambda'_0(x) dx = \int_0^{x_0} \lambda'_c(x) \lambda'_0(x) dx$$

$$a_0 \int_0^{x_0} \lambda'_0(x) \lambda'_1(x) dx + a_1 \int_0^{x_0} \lambda'_1(x) \lambda'_1(x) dx + a_2 \int_0^{x_0} \lambda'_2(x) \lambda'_1(x) dx + a_3 \int_0^{x_0} \lambda'_3(x) \lambda'_1(x) dx + a_4 \int_0^{x_0} \lambda'_4(x) \lambda'_1(x) dx + a_5 \int_0^{x_0} \lambda'_5(x) \lambda'_1(x) dx = \int_0^{x_0} \lambda'_c(x) \lambda'_1(x) dx$$

$$a_0 \int_0^{x_0} \lambda'_0(x) \lambda'_2(x) dx + a_1 \int_0^{x_0} \lambda'_1(x) \lambda'_2(x) dx + a_2 \int_0^{x_0} \lambda'_2(x) \lambda'_2(x) dx + a_3 \int_0^{x_0} \lambda'_3(x) \lambda'_2(x) dx + a_4 \int_0^{x_0} \lambda'_4(x) \lambda'_2(x) dx + a_5 \int_0^{x_0} \lambda'_5(x) \lambda'_2(x) dx = \int_0^{x_0} \lambda'_c(x) \lambda'_2(x) dx$$

$$a_0 \int_0^{x_0} \lambda'_0(x) \lambda'_3(x) dx + a_1 \int_0^{x_0} \lambda'_1(x) \lambda'_3(x) dx + a_2 \int_0^{x_0} \lambda'_2(x) \lambda'_3(x) dx + a_3 \int_0^{x_0} \lambda'_3(x) \lambda'_3(x) dx + a_4 \int_0^{x_0} \lambda'_4(x) \lambda'_3(x) dx + a_5 \int_0^{x_0} \lambda'_5(x) \lambda'_3(x) dx = \int_0^{x_0} \lambda'_c(x) \lambda'_3(x) dx$$

$$a_0 \int_0^{x_0} \lambda'_0(x) \lambda'_4(x) dx + a_1 \int_0^{x_0} \lambda'_1(x) \lambda'_4(x) dx + a_2 \int_0^{x_0} \lambda'_2(x) \lambda'_4(x) dx + a_3 \int_0^{x_0} \lambda'_3(x) \lambda'_4(x) dx + a_4 \int_0^{x_0} \lambda'_4(x) \lambda'_4(x) dx + a_5 \int_0^{x_0} \lambda'_5(x) \lambda'_4(x) dx = \int_0^{x_0} \lambda'_c(x) \lambda'_4(x) dx$$

$$a_0 \int_0^{x_0} \lambda'_0(x) \lambda'_5(x) dx + a_1 \int_0^{x_0} \lambda'_1(x) \lambda'_5(x) dx + a_2 \int_0^{x_0} \lambda'_2(x) \lambda'_5(x) dx + a_3 \int_0^{x_0} \lambda'_3(x) \lambda'_5(x) dx + a_4 \int_0^{x_0} \lambda'_4(x) \lambda'_5(x) dx + a_5 \int_0^{x_0} \lambda'_5(x) \lambda'_5(x) dx = \int_0^{x_0} \lambda'_c(x) \lambda'_5(x) dx$$

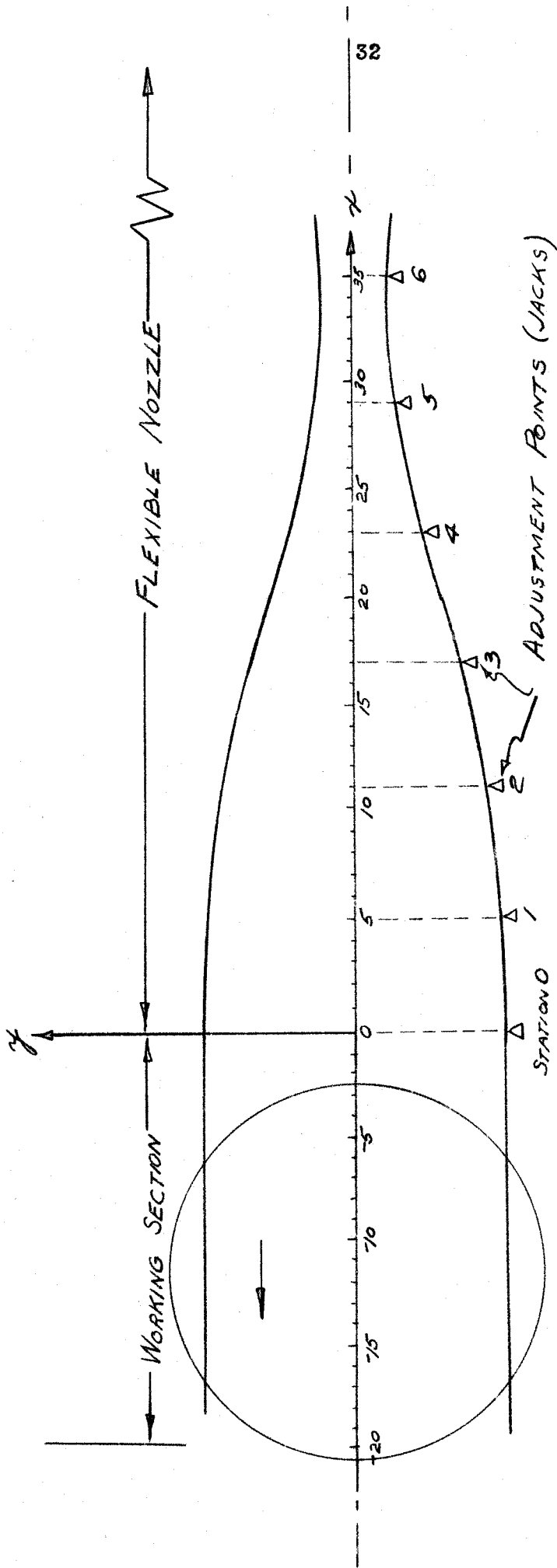
TABLE III

Numerical Simultaneous Equations for M = 2.537 NozzleJ.P.L. 12" Supersonic TunnelFirst Computation

$$\begin{aligned}
6.549a_0 - 0.447a_1 - 0.206a_2 + 4.522a_3 + 3.977a_4 - 0.755a_5 &= .00257 \\
- 0.447a_0 + 5.101a_1 - 1.071a_2 + 2.864a_3 + 5.598a_4 - 0.013a_5 &= .01210 \\
- 0.205a_0 - 1.071a_1 + 4.812a_2 - 0.517a_3 + 7.027a_4 + 0.317a_5 &= .00650 \\
4.522a_0 + 2.864a_1 - 0.517a_2 + 5.977a_3 + 7.752a_4 - 0.035a_5 &= .00447 \\
3.977a_0 + 5.598a_1 + 7.027a_2 + 7.752a_3 + 25.441a_4 + 0.268a_5 &= .02090 \\
- 0.755a_0 - 0.013a_1 + 0.317a_2 - 0.035a_3 + 0.268a_4 + 0.905a_5 &= .00050
\end{aligned}$$

Second Computation

$$\begin{aligned}
6.541a_0 - 0.447a_1 - 0.222a_2 + 4.521a_3 + 3.960a_4 - 0.817a_5 &= .00257 \\
- 0.447a_0 + 5.094a_1 - 1.069a_2 + 2.852a_3 + 5.597a_4 - 0.008a_5 &= .01000 \\
- 0.222a_0 - 1.069a_1 + 4.786a_2 - 0.515a_3 + 7.003a_4 + 0.321a_5 &= .00450 \\
4.521a_0 + 2.852a_1 - 0.515a_2 + 5.963a_3 + 7.748a_4 - 0.029a_5 &= .00453 \\
3.960a_0 + 5.597a_1 + 7.003a_2 + 7.748a_3 + 25.445a_4 + 0.305a_5 &= .02090 \\
- 0.817a_0 - 0.008a_1 + 0.321a_2 - 0.029a_3 + 0.305a_4 + 0.893a_5 &= .00003
\end{aligned}$$

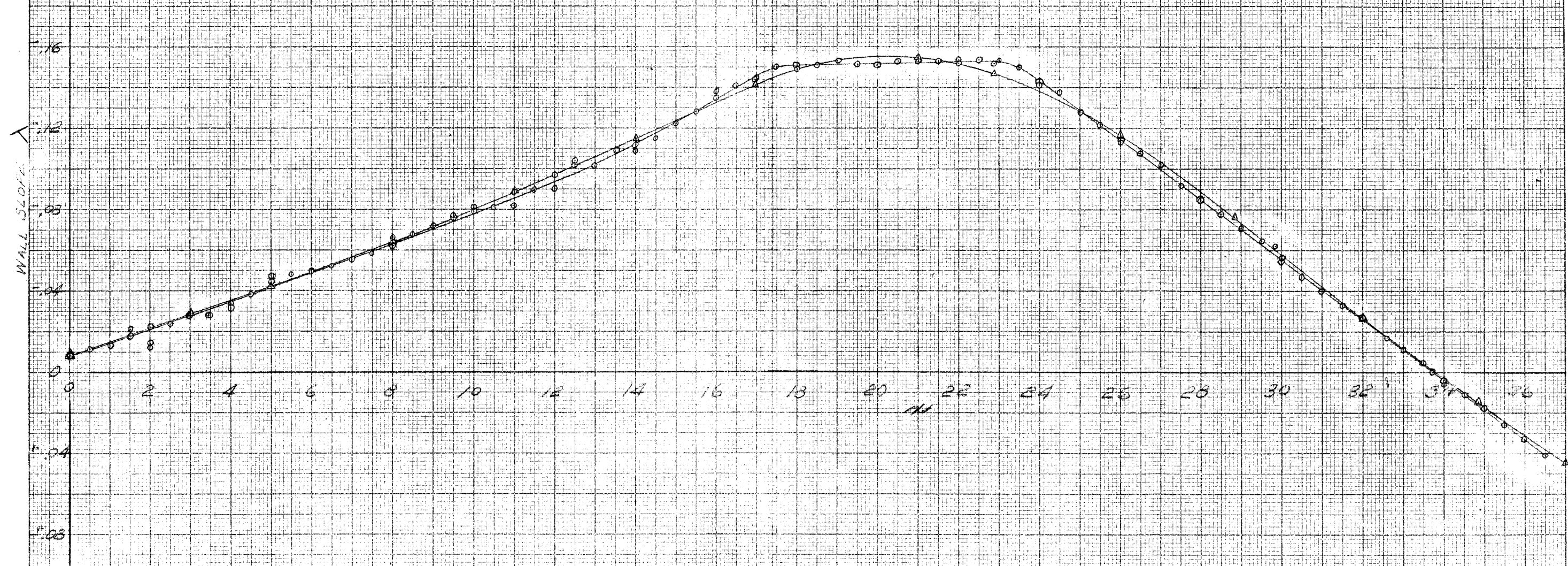


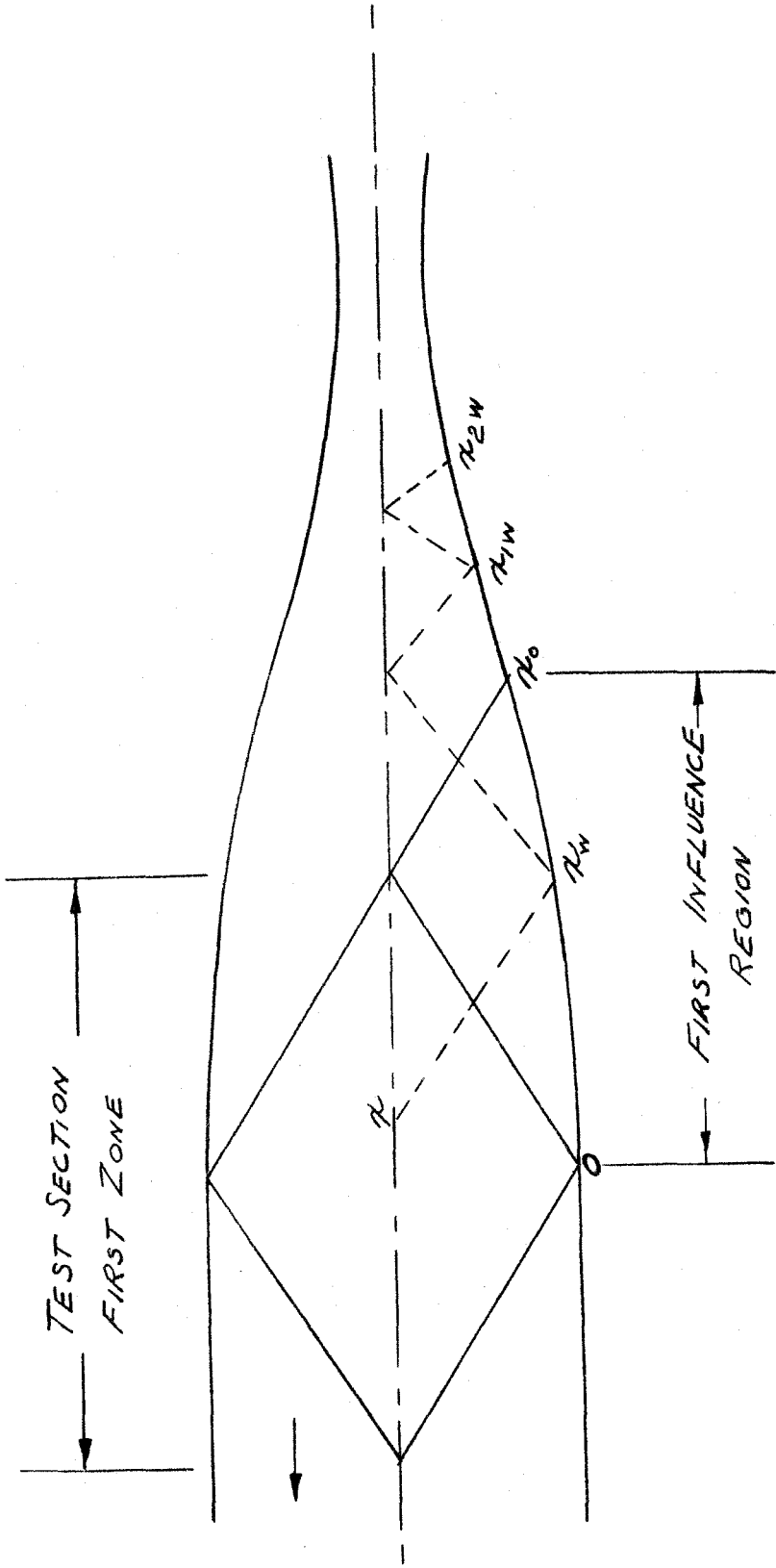
JPL 12" SUPERSONIC WIND TUNNEL CONFIGURATION

FIGURE 1

FIGURE 2
NOZZLE SLOPES

○ WALL SLOPE M=3.537A (THEORETICAL DESIGN)
△ " " " (ACTUAL ELASTIC)





INFLUENCE REGION AND MACH WAVES

FIGURE 3

FIGURE 4

INFLUENCE CURVES

λ_5 = INFLUENCE CURVE FOR
TWIST OF STATION 0

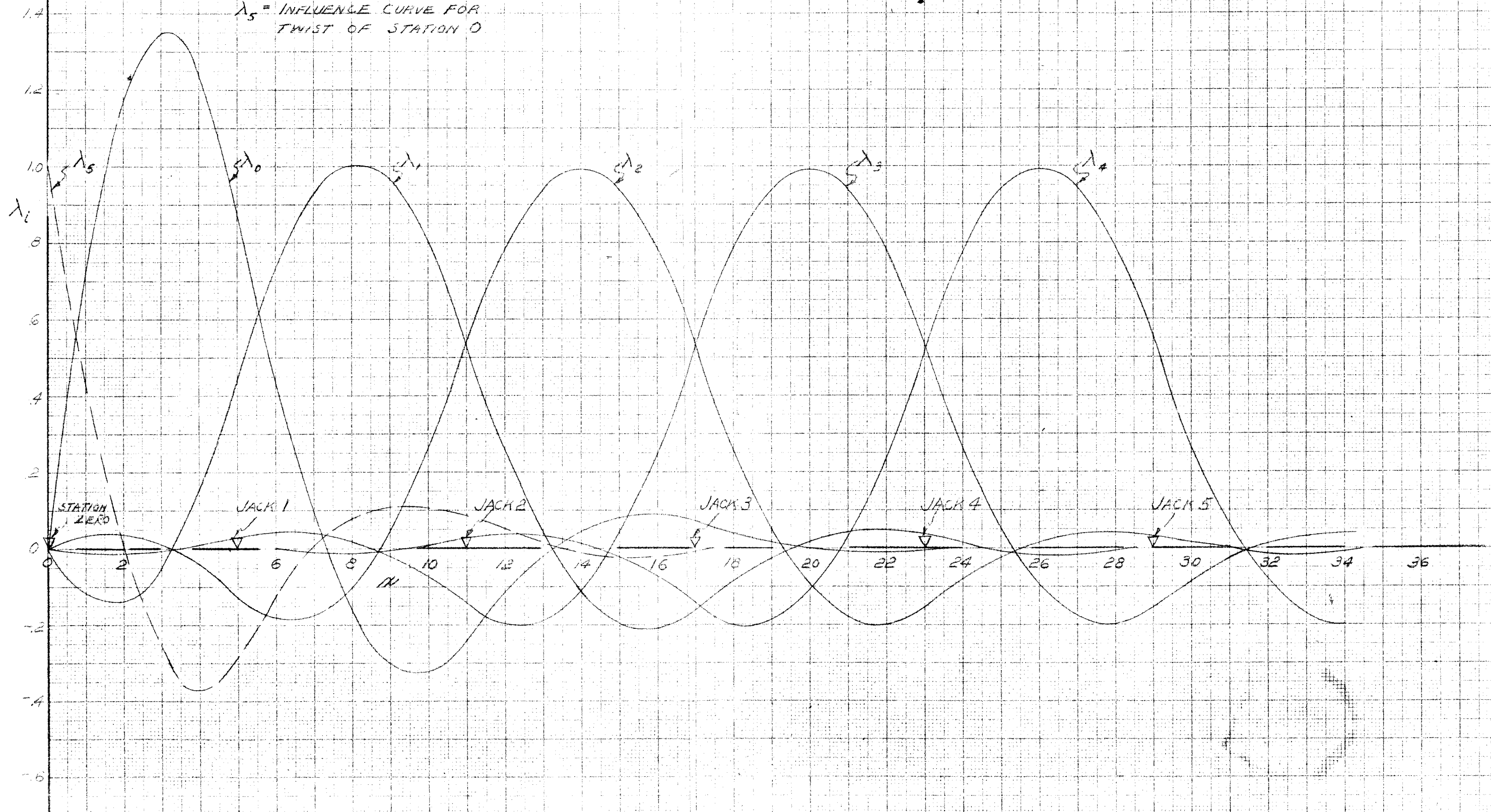


FIGURE 5
DESIRED SLOPE CORRECTION

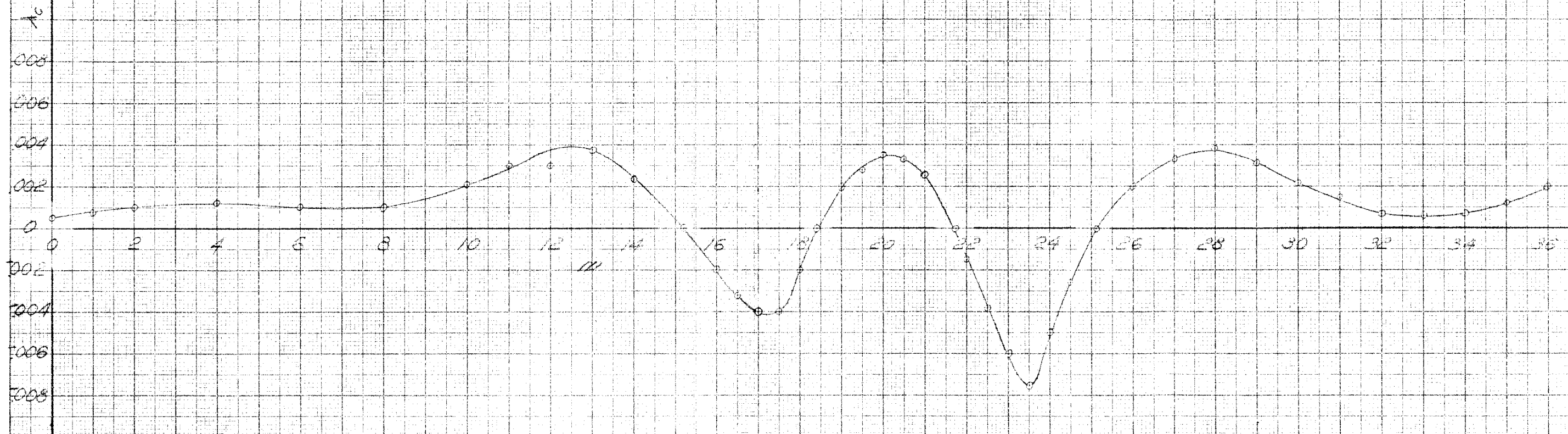


FIGURE 5
MACH WAVE REFLECTION
CURVES

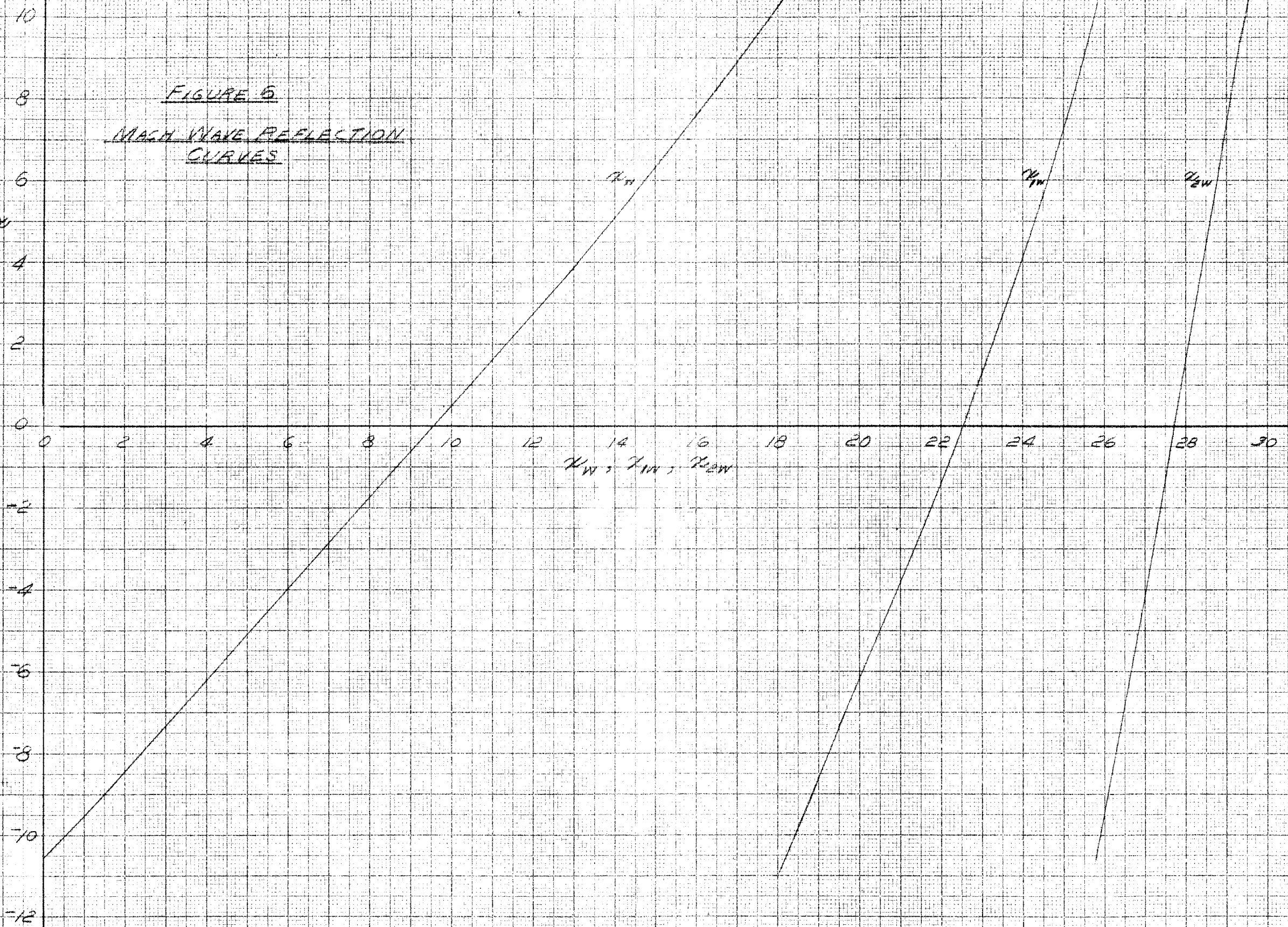
M

M_{11}

M_{12}

M_{21}

M_{11} M_{12} M_{21}



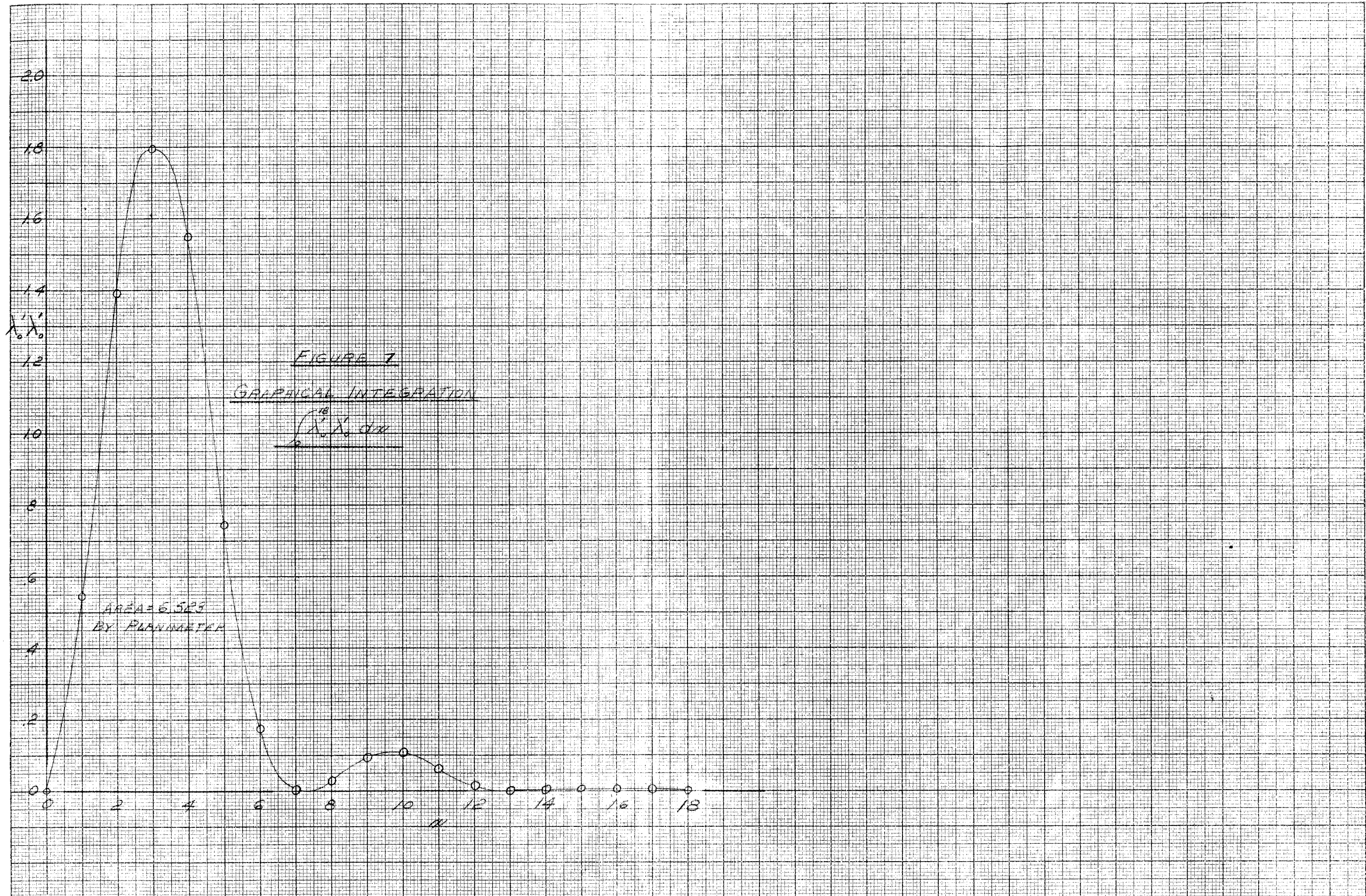


FIGURE 8

GRAPHICAL INTEGRATION

$\int_0^{13} X_1 X_2 dx$

AREA = .0068
BY PLANIMETER

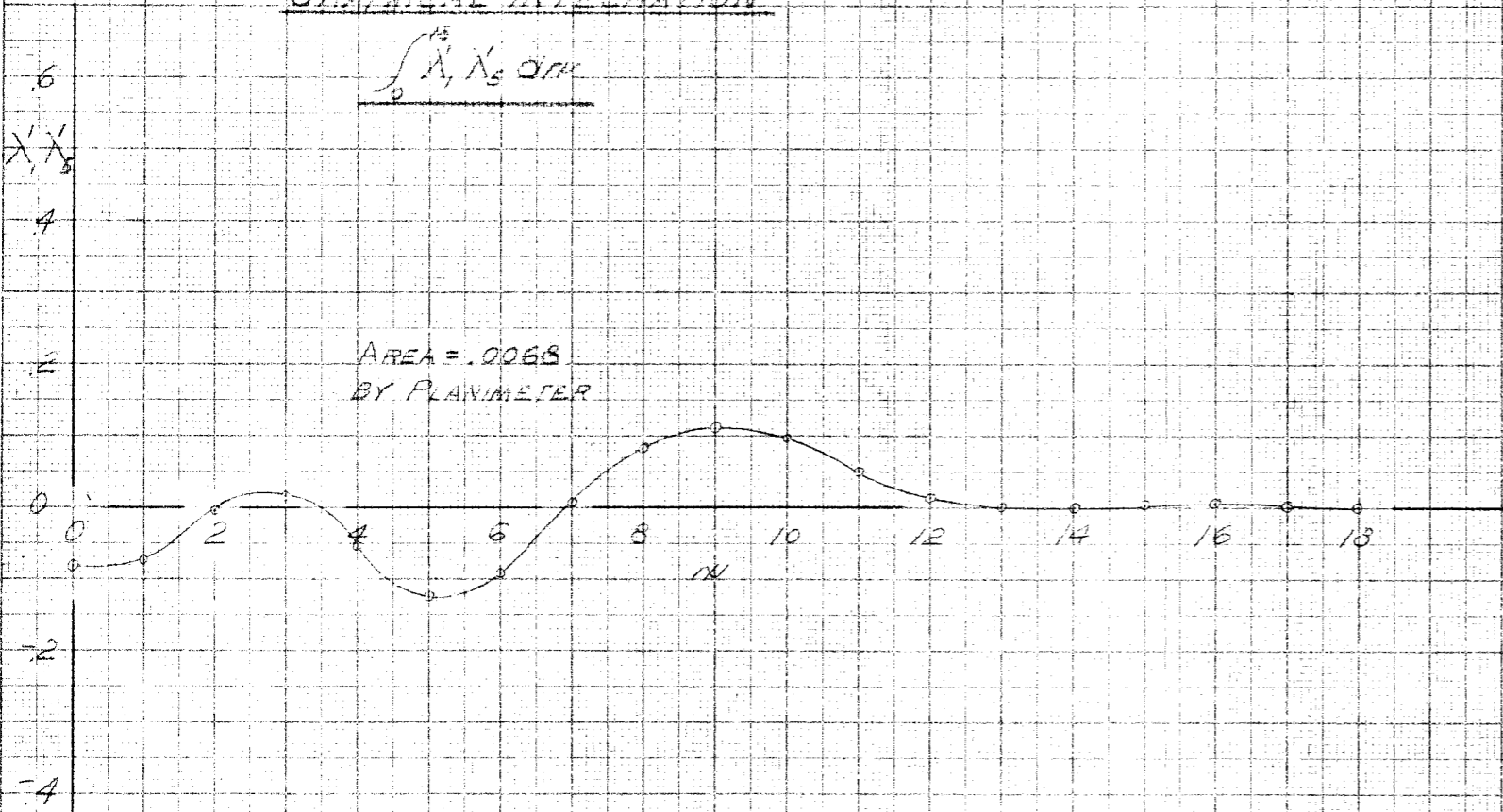


FIGURE 9

GRAPHICAL INTEGRATION

$$\int_0^{18} \lambda_2 \lambda_4 d\mu$$

AREA = 7.045
BY PLANIMETER

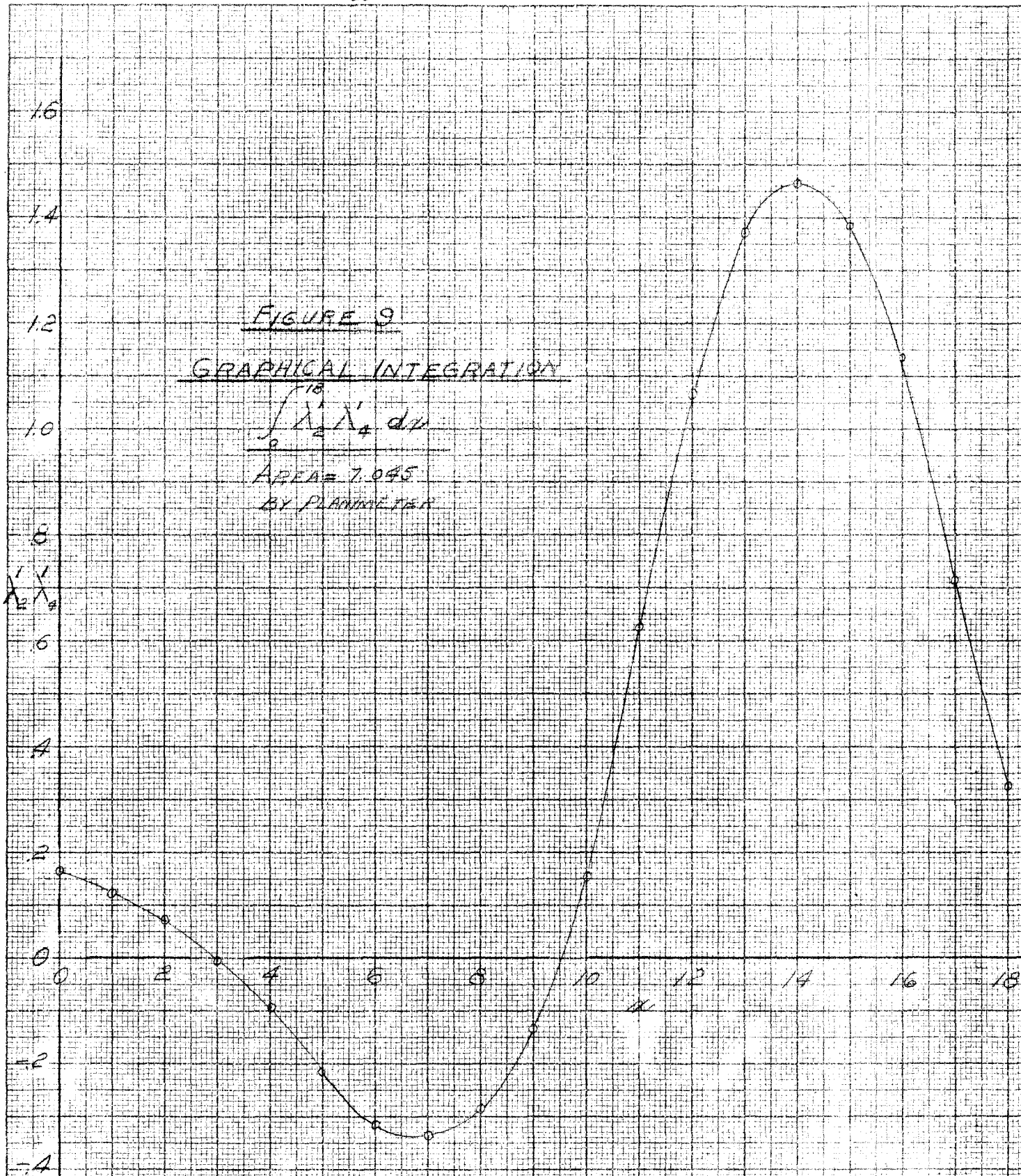


FIGURE 10
COMPARISON OF DESIRED SLOPE CORRECTION
AND THAT ACTUALLY OBTAINED

○ FIRST COMPUTATION OF OBTAINABLE CORRECTION
△ SECOND " " " " " "

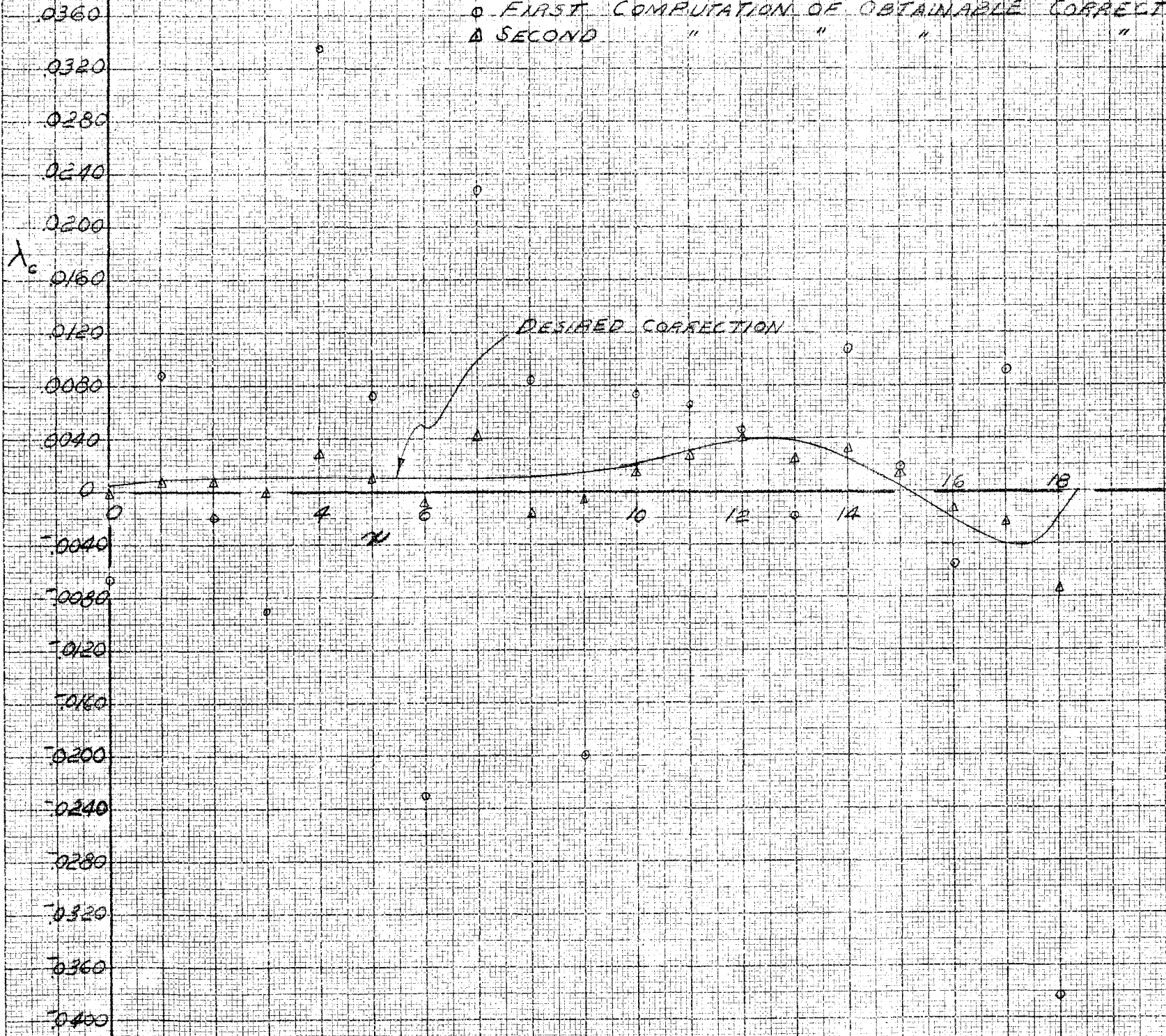
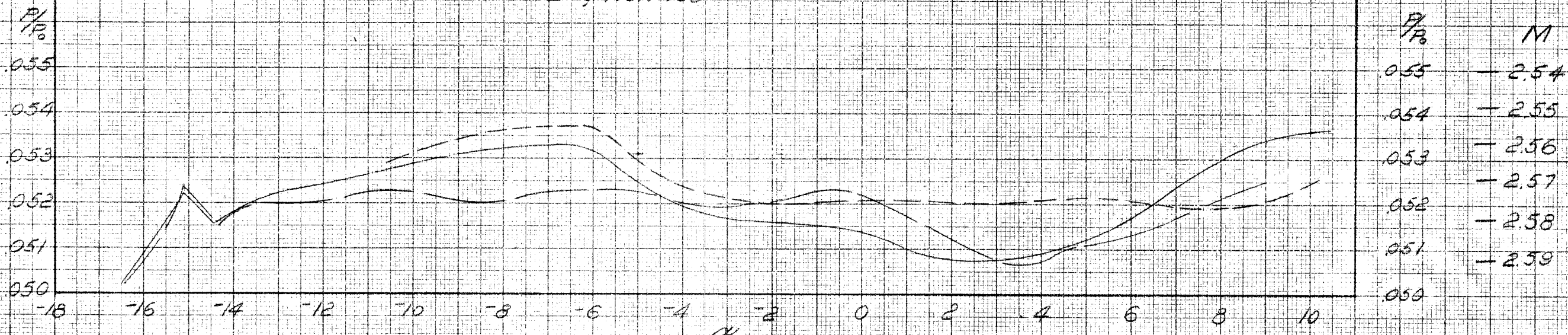


FIGURE II

PRESSURE DISTRIBUTION COMPARISON

————— EXPERIMENTAL, RUNS 93 AND 94
 - - - - - CORRECTED BY METHOD 1 (EIT HAD BEEN SUCCESSFUL)
 ————— " " " 2, RUN 103



ALUMINUM RESEARCH LABORATORIES
NEW KENSINGTON, PA.

AXIAL STRESS FATIGUE CURVES
FOR
76S-T6 ROD, 3/4-IN. DIAM

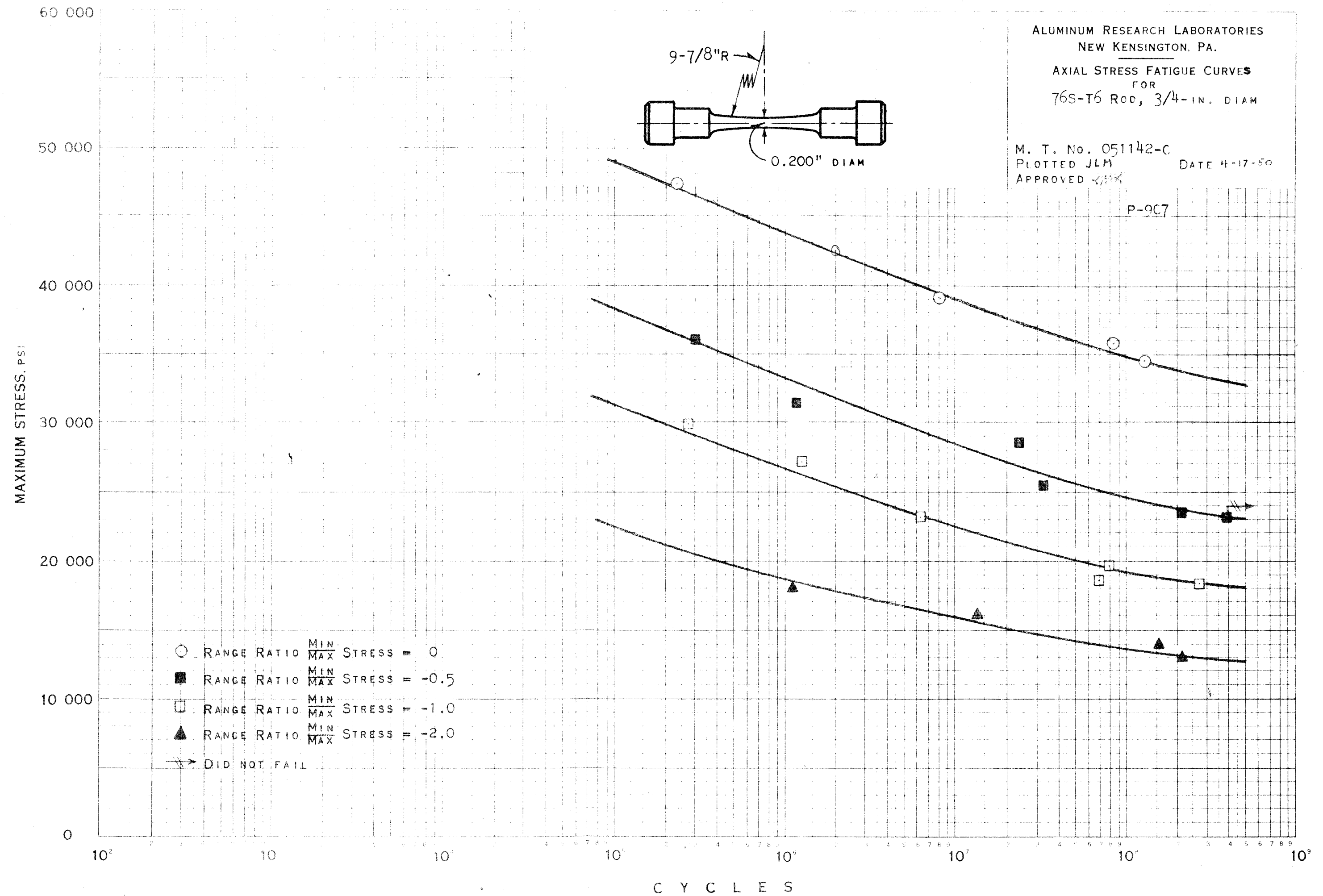
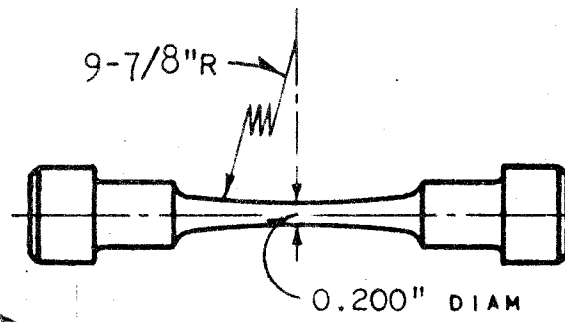
M. T. No. 051142-C

PLOTTED JLM

DATE 4-17-50

APPROVED *[Signature]*

P-907



- RANGE RATIO $\frac{\text{MIN}}{\text{MAX}}$ STRESS = 0
- RANGE RATIO $\frac{\text{MIN}}{\text{MAX}}$ STRESS = -0.5
- RANGE RATIO $\frac{\text{MIN}}{\text{MAX}}$ STRESS = -1.0
- ▲ RANGE RATIO $\frac{\text{MIN}}{\text{MAX}}$ STRESS = -2.0
- ↗ DID NOT FAIL